

Supporting Information

Assembly of Tetra-Nuclear Yb^{III}-Containing Selenotungstate Clusters: Synthesis, Structures, and Magnetic Properties

Li-Zhi Han,^a Cheng-Qi Jiao,^b Wei-Chao Chen,^{*c} Kui-Zhan Shao,^c Long-Yi Jin,^{*a} and Zhong-Min Su^a

^aDepartment of Chemistry, College of Science, Yanbian University, Yanji 133002, People's Republic of China

E-mail: lyjin@ybu.edu.cn

^bLiaoning Normal University Liaoning Normal Univ, Sch Chem & Chem Engn, Huanghe Rd 850, Dalian 116029, Peoples R China

^cKey Laboratory of Polyoxometalate and Reticular Material Chemistry of Ministry of Education, Northeast Normal University Ren Min Street No. 5268 Changchun, Jilin, 130024 P. R. China

E-mail: chenwc061@nenu.edu.cn

CONTENTS

Section 1 A detailed survey of the lanthanoid-containing selenotungstates

Section 2 Structures

Section 3 Experimental Section

Section 4 Supplementary Physical Characterizations

Section 1 A detailed survey of the lanthanoid-containing selenotungstates

Table S1. A detailed survey of the lanthanoid-containing selenotungstates.

Year	Lanthanoid ions	Formula	properties	Ref.
2013	Ce	$K_{32}Na_{16}\{(SeO_3)W_{10}O_{34}\}_8\{Ce_8(H_2O)_{20}\}(WO_2)_4(W_4O_{12})\cdot81H_2O$ $K_{32}Na_{16}\{(TeO_3)W_{10}O_{34}\}_8\{Ce_8(H_2O)_{20}\}(WO_2)_4(W_4O_{12})\cdot114H_2O$ $K_{12}Na_{22}\{(SeO_3)W_{10}O_{34}\}_8\{Ce_8(H_2O)_{20}\}(WO_2)_4\{(W_4O_6)Ce_4(H_2O)_{14}(SeO_3)_4(NO_3)_2\}\cdot79H_2O$	the formation of inorganic hollow spheres in dilute solution	1
2014	Ce	$(C_2H_8N)_4K_3Na_{10}[(\alpha-SeW_9O_{33})_2\{Ce_2(CH_3COO)(H_2O)_3W_3O_6\}(\alpha-Se_2W_{14}O_{52})]\cdot26H_2O;$ $K_{10}Na_5[(\alpha-SeW_9O_{33})_2\{Ce_2(H_2O)_4W_3O_6\}(\alpha-Se_2W_{14}O_{51}(OH))]\cdot24H_2O$	DFT for the investigations of electronic properties	2
2015	Ce	$K_6Na_{16}[Ce_6Se_6W_{67}O_{230}(OH)_6(H_2O)_{17}]\cdot47H_2O;$ $K_9Na_5Ce(H_2O)_4[Ce_6Se_{10}W_{51}O_{187}(OH)_7(H_2O)_{18}]\cdot45H_2O$	electrochemical properties	3
2015	Ce	$Na_{13}H_7[Ce(SeW_{17}O_{59})_2]\cdot31H_2O$	electrochemical properties	4
2017	La, Ce	$[H_2N(CH_3)_2]_{16}Na_9LnH_{10}\{[W_{16}Ln_{10}(H_2O)_{38}O_{50}][B-\alpha-SeW_9O_{33}]_8\}\cdot56H_2O;$ $[H_2N(CH_3)_2]_{22}Na_4H_{12}\{[W_{18}Ln_{10}(H_2O)_{34}O_{56}][B-\alpha-SeW_9O_{33}]_8\}\cdot80H_2O$	variable-temperature IR spectra and PXRD patterns	5
2017	Pr	$Cs_2Na_4H_{12}\{[Pr_3(H_2O)_{10}[Se_2W_{22}O_{76}(gly)_2]\}_2(Se_2W_7O_{30}H_2)\}\cdot25H_2O$	H_2O_2 -based catalytic epoxidation property	6
2018	Tb, Dy	$[H_2N(CH_3)_2]_2Na_9K_2H_{19}\{[Ln_4W_4Se_4O_{22}(H_2O)_5](Se_2W_{14}O_{52})_2\}\cdot60H_2O$	solid-state luminescent spectra	7
2019	Gd, Dy	$[H_2N(CH_3)_2]_{10}H_3[SeO_4Ln_5(H_2O)_7(Se_2W_{14}O_{52})_2]\cdot40H_2O$	luminescence properties	8
2019	Ce	$[HDMEA][H_2N(CH_3)_2]_4H_3Na_4[Ce_2(H_2O)_6(DMEA)W_4O_9(\alpha-SeW_9O_{33})_3]\cdot26H_2O;$ $[H_2N(CH_3)_2]_{10}H_4Na_{10}[Ce_2W_4O_9(H_2O)_7(\alpha-SeW_9O_{33})_3]\cdot2\cdot63H_2O$	the oxidation of aromatic sulfides	9
2019	Gd, Tb, Dy	$(C_4H_{10}NO)_9Na_3[Dy_3Se_{3.5}W_{30}O_{107.5}(H_2O)_{10}]\cdot22H_2O;$ $(NH_4)_3(C_2H_8N)Na_2[Dy_4Se_6W_{38}O_{132}(H_2O)_{26}(OH)_6]\cdot18H_2O;$ $(NH_4)_4Na_8[Gd_4Se_6W_{48}O_{166}(H_2O)_{20}(OH)_4]\cdot21H_2O;$ $(NH_4)_9(C_2H_8N)_4Na_5[Ln_6Se_6W_{58}O_{202}(H_2O)_{20}(OH)_4]\cdot58H_2O;$ $(NH_4)_4(C_2H_8N)_5Na_{13}[Ln_4Se_8W_{56}O_{196}(H_2O)_x(OH)_{10}]\cdot40H_2O$	magnetic behaviors	10

2020	Ho, Er, Tb, Tm	[H ₂ N(CH ₃) ₂] ₁₀ H ₃ [SeO ₄ Ln ₅ (H ₂ O) ₇ (Se ₂ W ₁₄ O ₅₂) ₂]·40H ₂ O	luminescence properties	11
2020	Nd	Na ₉ K ₈ {[W ₃ Nd ₂ (H ₂ O) ₃ (NO ₃)O ₆](B- α -SeW ₉ O ₃₃) ₂ (α -Se ₂ W ₁₄ O ₅₂)} ₃ ·35H ₂ O; [H ₂ N(CH ₃) ₂] ₇ H ₉ Na ₄ {[W ₂ Nd ₂ (H ₂ O) ₈ O ₆ (OH) ₂ (β -Se ₂ W ₁₄ O ₅₂)][W ₃ Nd ₂ (H ₂ O) ₆ O ₇ (B- α -SeW ₉ O ₃₃) ₂]} ₂ }·84H ₂ O	catalytic oxidation of aromatic thioethers	12
2020	Eu	[H ₂ N(CH ₃) ₂] ₁₀ H ₃ [SeO ₄ Eu ₅ (H ₂ O) ₈ [Se ₂ W ₁₄ O ₅₂] ₂]·40H ₂ O	luminescence properties	13
2020	Ce, Pr, Nd, Sm, Gd, Tb, Ho, Er	[H ₂ N(CH ₃) ₂] ₁₂ Na ₂ [Ln ₂ (H ₂ O) ₇ (W ₄ O ₉)(HPSeW ₁₅ O ₅₄)(SeW ₉ O ₃₃) ₂] ₂ ·44H ₂ O	electrochemical sensing properties	14
2020	Ce	Na ₁₆ H ₆ {[Ce ₃ W ₄ O ₁₀ (H ₂ O) ₉ (CH ₃ COO) ₃] ₂ (Se ₂ W ₇ O ₃₀)(B- α -SeW ₉ O ₃₃) ₄ }(C ₅ H ₈ NBO ₃)·119H ₂ O	electrochemical sensing properties	15
2021	Yb	(C ₂ H ₈ N) ₆ Na ₁₄ [Yb ₄ Se ₆ W ₄₄ O ₁₆₀ (H ₂ O) ₁₂] ₂ ·40H ₂ O; (C ₂ H ₈ N) ₄ Na ₁₄ [Yb ₄ Se ₆ W ₄₅ O ₁₅₉ (OH) ₆ (H ₂ O) ₁₁] ₂ ·38H ₂ O	single molecule magnets	This work

REFERENCES

- (1) Chen, W.-C.; Li, H.-L.; Wang, X.-L.; Shao, K.-Z.; Su, Z.-M.; Wang, E.-B. Assembly of cerium(III)-stabilized polyoxotungstate nanoclusters with SeO₃²⁻/TeO₃²⁻ templates: from single polyoxoanions to inorganic hollow spheres in dilute solution. *Chem. Eur. J.* **2013**, *19*, 11007-11015.
- (2) Chen, W.-C.; Yan, L.-K.; Wu, C.-X.; Wang, X.-L.; Shao, K.-Z.; Su, Z.-M.; Wang, E.-B. Assembly of Keggin-/Dawson-type polyoxotungstate clusters with different metal units and SeO₃²⁻ heteroanion templates. *Cryst. Growth Des.* **2014**, *14*, 5099-5110.
- (3) Chen, W.-C.; Qin, C.; Li, Y.-G.; Zang, H.-Y.; Shao, K.-Z.; Su, Z.-M.; Wang, E.-B. Assembly of large purely inorganic Ce-stabilized/bridged selenotungstates: from nanoclusters to layers. *Chem. Asian J.* **2015**, *10*, 1184-1191.
- (4) Li, H.; Yang, W.; Chai, Y.; Chen, L.; Zhao, J. A novel Dawson-like cerium(IV)-hybridizing selenotungstate Na₁₃H₇[Ce(SeW₁₇O₅₉)₂]₂·31H₂O. *Inorg. Chem. Commun.* **2015**, *56*, 35-40.
- (5) Liu, Y.; Li, H.; Lu, C.; Gong, P.; Ma, X.; Chen, L.; Zhao, J. Organocounterions-assisted and pH-controlled self-assembly of five nanoscale high-Nuclear lanthanide substituted heteropolytungstates. *Cryst. Growth Des.* **2017**, *17*, 3917-3928.
- (6) Yang, L.; Li, L.; Guo, J.; Liu, Q.; Ma, P.; Niu, J.; Wang, J. A nanosized gly-decorated praseodymium-stabilized selenotungstate cluster: synthesis, structure, and oxidation catalysis. *Chem. Asian J.* **2017**, *12*, 2441-2446.
- (7) Li, H.-L.; Liu, Y.-J.; Li, Y.-M.; Chen, L.-J.; Zhao, J.-W.; Yang, G.-Y. Unprecedented selenium and lanthanide simultaneously bridging selenotungstate aggregates stabilized by four tetravacant Dawson-like {Se₂W₁₄} units. *Chem. Asian J.* **2018**, *13*, 2897-2907.
- (8) Y. Zhang, Y. Li, J. Pang, Y. Liu, P. Li, L. Chen and J. Zhao, Two Penta-RE^{III} Encapsulated Tetravacant Dawson Selenotungstates and Nanoscale Derivatives and Their Luminescence Properties, *Inorg. Chem.* **2019**, *58*, 7078-7090.
- (9) Li, H.-L.; Lian, C.; Chen, L.-J.; Zhao, J.-W.; Yang, G.-Y. Two Ce³⁺-substituted selenotungstates regulated by N,N-dimethylethanolamine and dimethylamine hydrochloride, *Inorg. Chem.* **2019**, *58*, 8442-8450.

- (10) W.-C. Chen, C.-Q. Jiao, X.-L. Wang, K.-Z. Shao and Z.-M. Su, Self-Assembly of Nanoscale Lanthanoid-Containing Selenotungstates: Synthesis, Structures, and Magnetic Studies, *Inorg. Chem.* **2019**, *58*, 12895–12904.
- (11) Y. Zhang, Y.-F. Liu, X. Xu, L.-J. Chen and J.-W. Zhao, Preparations, Structures and Luminescence Properties of Pentarare-earth Incorporated Tetravacant Dawson Selenotungstates and Their Ho³⁺/Tm³⁺ Co-doped Derivatives, *Chem Asian J.* **2020**, *15*, 1156–1166.
- (12) H. Li, C. Lian, L. Chen, J. Zhao and G.-Y. Yang, Two unusual nanosized Nd³⁺-substituted selenotungstate aggregates simultaneously comprising lacunary Keggin and Dawson polyoxotungstate segments, *Nanoscale*, **2020**, *12*, 16091–16101.
- (13) Y. Zhang, B. Zeng, Y. Liu, P. Li, L. Chen and J. Zhao, A Penta-Eulli Sandwiched Dawson Selenotungstate and Its Unique Luminescence Properties, *Eur. J. Inorg. Chem.* **2020**, 3416–3425.
- (14) L. Liu, J. Jiang, X. Liu, G. Liu, D. Wang, L. Chen and J. Zhao, First series of mixed (P^{III}, Se^{IV})-heteroatomoriented rare-earth-embedded polyoxotungstates containing distinct building blocks, *Inorg. Chem. Front.*, **2020**, *7*, 4640–4651.
- (15) J. Jiang, L. Liu, G. Liu, D. Wang, Y. Zhang, L. Chen and J. Zhao, Organic-Inorganic Hybrid Cerium-Encapsulated Selenotungstate Including Three Building Blocks and Its Electrochemical Detection of Dopamine and Paracetamol, *Inorg. Chem.* **2020**, *59*, 15355–15364.

Section 2 Structures

Table S2. Crystal Data and Structure Refinements for **1** and **2**.

	1	2
Empirical formula	$C_{12}H_{152}N_6Na_{14}O_{212}Se_6W_{44}Yb_4$	$C_8H_{136}N_4Na_{14}O_{214}Se_6W_{45}Yb_4$
M	13350.57	13474.23
$\lambda/\text{\AA}$	0.71073	0.71073
T/K	296.15	296.15
Crystal system	Orthorhombic	Triclinic
Space group	$Pbcn$	$P-1$
$a/\text{\AA}$	50.919(2)	17.1503(13)
$b/\text{\AA}$	23.3103(8)	25.581(2)
$c/\text{\AA}$	20.2832(8)	35.869(3)
$\alpha/^\circ$	90	93.152(2)
$\beta/^\circ$	90	99.869(2)
$\gamma/^\circ$	90	106.340(2)
$V/\text{\AA}^3$	24074.8(16)	14788(2)
Z	4	2
$D_c/\text{Mg m}^{-3}$	3.683	3.026
μ/mm^{-1}	23.499	19.514
$F(000)$	23424	11784
2θ Range/ $^\circ$	3.584–49.998	2.954–43.492
Measured reflections	135589	62674
Independent reflections	21189	34925
R_{int} after SQUEEZE	0.1655	0.0963
Goodness-of-fit on F^2	1.029	1.018
$R_1(I > 2\sigma(I))^a$	0.0552	0.0756
wR_2 (all data) ^b	0.1392	0.2282

^a $R_1 = \sum |F_o| - |F_c| | / \sum |F_o|$. ^b $wR_2 = \{\sum [w(F_o^2 - F_c^2)^2] / \sum [w(F_o^2)^2]\}^{1/2}$.

Single-crystal X-ray diffraction: Single-crystal X-ray diffraction data for **1** and **2** were recorded on a Bruker Apex CCD II area-detector diffractometer with graphite-monochromated Mo_{Kα} radiation ($\lambda = 0.71073 \text{ \AA}$) at 296(2) K. Absorption corrections were applied using multi-scan technique and performed by using the SADABS program (Sheldrick, G. *SADABS*; ver. 2.10; University of Gottingen: Göttingen, Germany, 2003). The structures of **1** and **2** were solved by direct methods and refined on F^2 by full-matrix leastsquares methods by using the Olex2 package (*J. Appl. Cryst.*, 2009, 42, 339). CCDC number: 2067697 for **1**; 2067696 for **2**.

As for CCDC 2067696, about one Na⁺ and 3 [C₂H₈N]⁺ cations as well as 5 water molecules were found from the Fourier maps, however, there are still accessible solvent voids in the crystal structure prompted by Checkcif report, indicating that some more cations and solvent molecules should exist in the structure, but cannot be found from the weak residual electron peaks. Based on the TGA curve, bond valence sum calculations, elemental analyses, another 33 water molecules, 13 Na⁺, one [C₂H₈N]⁺ cation and 34 H⁺ were included into the molecular formula directly. Specifically, the 38 water molecules and 4 organic amine groups in this formula were confirmed by TGA curve, two successive weight decrease is the loss of water molecules and organic amine groups (Cacl: 7.91%; Found: 7.82%). Elemental analysis supports this molecular formula once again (Cacl: C 0.71, N 0.42, Na 2.39, Yb 5.14, Se 3.52, W 61.4 %; Found C 0.69, N 0.50, Na 2.88, Yb 5.06, Se 3.49, W 60.8 %). In all, the molecular formula was defined as (C₂H₈N)₄Na₁₄[Yb₄Se₆W₄₅O₁₅₉(OH)₆(H₂O)₁₁]·38H₂O according to single crystal analysis, charge balance, TGA curve as well as elemental analyses.

As for CCDC 2067697, about one Na⁺ and 4 [C₂H₈N]⁺ cations as well as 9 water molecules were found from the Fourier maps, however, there are still accessible solvent voids in the crystal structure prompted by Checkcif report, indicating that some more cations and solvent molecules should exist in the structure, but cannot be found from the weak residual electron peaks. Based on the TGA curve, bond valence sum calculations, elemental analyses, another 31 water molecules, 13 Na⁺, 2 [C₂H₈N]⁺ cations and 40 H⁺ were included into the molecular formula directly. Specifically, the 40 water molecules and 6 organic amine groups in this formula were confirmed by TGA curve, two successive weight decrease is the loss of water molecules and organic amine groups (Cacl: 9.08%; Found: 8.93%). Elemental analysis supports this molecular formula once again (Cacl: C 1.08, N 0.63, Na 2.41, Yb 5.18, Se 3.55, W 60.6 %; Found C 0.98, N 0.67, Na 2.98, Yb 5.13, Se 3.31, W 59.9 %). In all, the molecular formula was defined as (C₂H₈N)₆Na₁₄[Yb₄Se₆W₄₄O₁₆₀(H₂O)₁₂]·40H₂O according to single crystal analysis, charge balance, TGA curve as well as elemental analyses.

Table S3. Bond lengths [Å] for the Yb atoms in **1–2**.

1			
Yb(1)-O(8)	2.382(15)	Yb(2)-O(34)	2.273(15)
Yb(1)-O(16)	2.302(15)	Yb(2)-O(40)	2.385(16)
Yb(1)-O(25)	2.339(15)	Yb(2)-O(51)	2.292(16)
Yb(1)-O(30)	2.316(15)	Yb(2)-O(69)	2.317(15)
Yb(1)-O(53)	2.314(17)	Yb(2)-O(73)	2.314(17)
Yb(1)-O(70)	2.283(16)	Yb(2)-O(81)	2.321(16)
Yb(1)-O(79)	2.337(16)	Yb(2)-O(82)	2.311(16)
Yb(1)-O(80)	2.346(17)	Yb(2)-O(83)	2.370(18)
2			
Yb(1)-O(22)	2.26(3)	Yb(2)-O(2)	2.23(3)
Yb(1)-O(44)	2.19(2)	Yb(2)-O(35)	2.29(3)
Yb(1)-O(50)	2.30(3)	Yb(2)-O(37)	2.35(4)
Yb(1)-O(95)	2.30(3)	Yb(2)-O(110)	2.25(3)
Yb(1)-O(117)	2.21(4)	Yb(2)-O(123)	2.24(3)
Yb(1)-O(145)	2.36(4)	Yb(2)-O(174)	2.34(3)
Yb(1)-O(159)	2.27(2)	Yb(2)-O(154)	2.34(3)
Yb(3)-O(65)	2.27(3)	Yb(4)-O(20)	2.27(3)
Yb(3)-O(67)	2.20(4)	Yb(4)-O(22)	2.15(3)
Yb(3)-O(69)	2.35(4)	Yb(4)-O(63)	2.29(4)
Yb(3)-O(75)	2.42(4)	Yb(4)-O(77)	2.29(3)
Yb(3)-O(96)	2.26(3)	Yb(4)-O(84)	2.28(3)
Yb(3)-O(123)	2.12(3)	Yb(4)-O(136)	2.26(3)
Yb(3)-O(149)	2.35(3)	Yb(4)-O(162)	2.27(3)

Table S4. The BVS calculation results of all the oxygen atoms in **2**.

Oxygen Code	Bond Valence	Protonation Degree	Oxygen Code	Bond Valence	Protonation Degree
O ₁₅	1.349	1	O ₁₀₉	1.422	1
O ₁₅₆	1.372	1	O ₁₀₅	0.355	2
O ₇₃	1.372	1	O ₁₂₃	0.778	1
O ₂₂	0.737	1			
Total 8 protons per cluster					

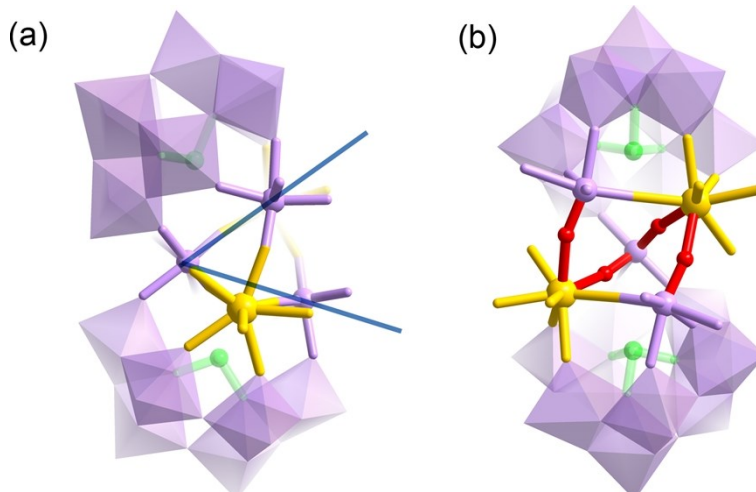


Fig. S1 The twist angle (a) and four Yb-O-W linkages (b, red bonds) in dimeric $\{\text{Yb}_2\text{Se}_2\text{W}_{21}\}$ subunit. Color code: W (purple); Se (green); Yb (yellow).

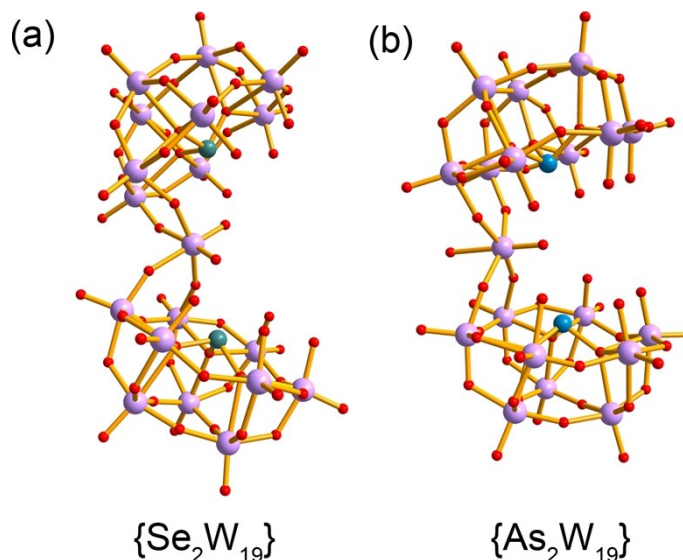


Fig. S2 The open pocket-like fragments of $[\text{Se}_2\text{W}_{19}\text{O}_{68}]^{14-}$ (a) and $[\text{As}_2\text{W}_{19}\text{O}_{68}]^{16-}$ (b). Color code: W (purple); Se or As (blue); O (red).

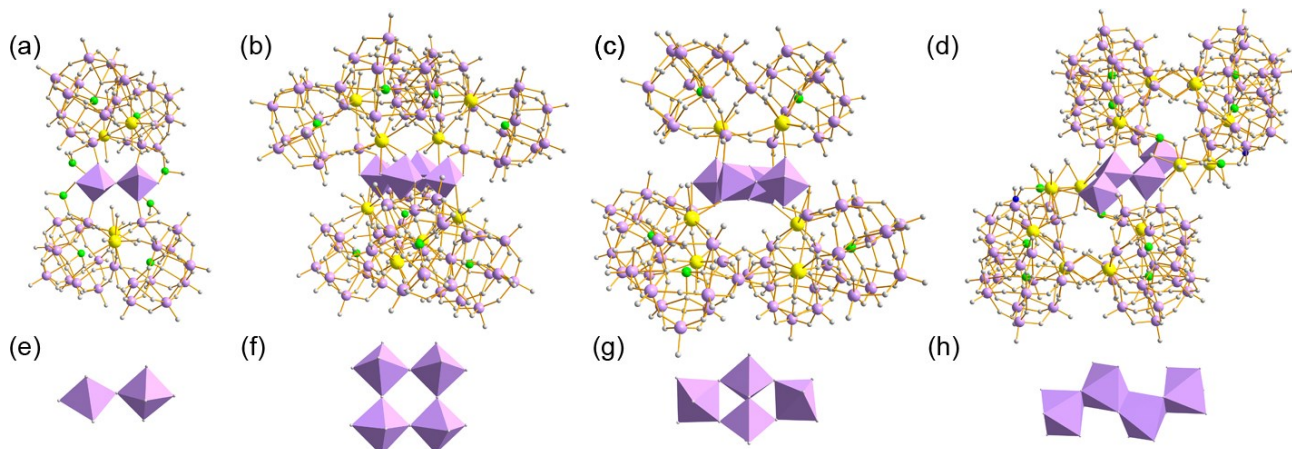


Fig. S3 Dimeric (a), trimeric (c) or tetrameric (b,d) Ln-containing selenotungstates based on three or four $\{Yb_2Se_2W_{21}\}$ subunits fixed by $\{W_2O_7\}$ (e) or $\{W_4\}$ linkers (f, g and h), respectively. Color code: W (purple); Se (green); Yb or Ce (yellow); O (gray).

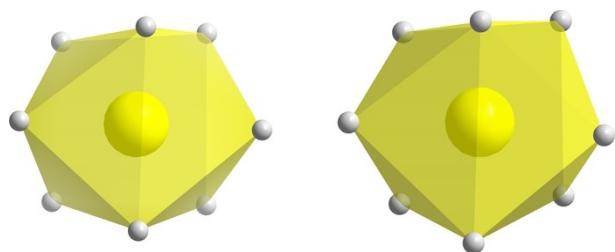


Fig. S4 The distorted square antiprismatic geometries of Yb^{III} centers. Color code: Yb (yellow); O (gray).

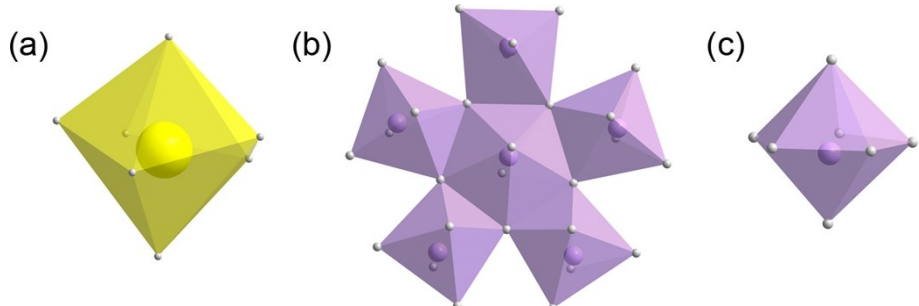


Fig. S5 The pentagonal bipyramidal geometry of Yb center (a) and molybdenum $\{Mo(Mo_5)\}$ or tungsten $\{W(W_5)\}$ centers (b,c). Color code: W or Mo (purple); Yb (yellow); O (gray).

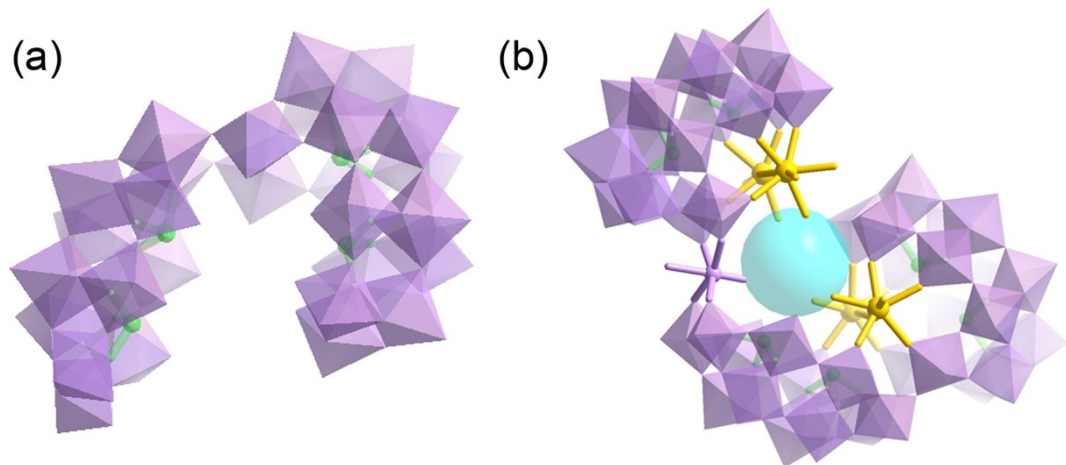


Fig. S6 Polyhedral and ball-and-stick representation of opening {Se₄W₂₈} subunit (a) and the “cavity” in **2a** with a half-“S”-shaped configuration (b). Color code: W (purple); Se (green); Yb (yellow).

Table S5. Lanthanide geometry analysis of **1** by using the Shape software.

Ideal shape	Octagon	Heptagonal pyramid	Hexagonal bipyramid	Cube	Square antiprism	Triangular dodecahedron	Johnson gyrobifastigium	Johnson elongated triangular bipyramid	Biaugmented trigonal prism	Biaugmented trigonal prism	Snub diphenoид	Triakis tetrahedron	Elongated trigonal bipyramid
Abbreviation	OP-8	HPY-8	HBPY-8	CU-8	SAPR-8	TDD-8	JGBF-8	JETPY-8	JBTPR-8	BTPR-8	JSD-8	TT-8	ETBPY-8
Symmetry	D_{8h}	C_{7v}	D_{6h}	O_h	D_{4d}	D_{2d}	D_{2d}	D_{3h}	C_{2v}	C_{2v}	D_{2d}	T_d	D_{3h}
$CShM_{(Yb1)}$	30.795	23.452	15.768	9.149	0.908	0.964	15.191	29.559	1.975	1.545	3.511	9.837	24.776
$CShM_{(Yb2)}$	31.209	23.042	16.265	10.208	1.046	1.348	14.398	29.538	1.854	1.467	3.696	10.822	24.783

Table S6. Lanthanide geometry analysis of **2** by using the Shape software.

Ideal shape	Heptagon	Hexagonal pyramid	Pentagonal bipyramid	Capped octahedron	Capped trigonal prism	Johnson pentagonal bipyramid	Johnson triangular pyramid
Abbreviation	HP-7	HPY-7	PBPY-7	COC-7	CTPR-7	JPBPY-7	JETPY-7
Symmetry	D_{7h}	C_{6v}	D_{5h}	C_{3v}	C_{2v}	D_{5h}	C_{3v}
$CShM_{(Yb1)}$	29.927	20.493	5.498	2.386	0.765	8.827	18.763
$CShM_{(Yb2)}$	34.464	22.027	1.691	4.221	3.412	5.729	21.098
$CShM_{(Yb3)}$	35.093	22.436	1.654	4.566	3.634	5.283	20.054
$CShM_{(Yb4)}$	28.923	20.508	6.730	2.202	0.709	10.097	18.401

Section 3 Experimental Section

Materials and Characterization: All chemicals and solvents were commercially purchased and used without further purification. C and N were performed on a PerkinElmer 2400 CHN elemental analyzer. Elemental analysis of Na, Yb, Se, and W were performed with a Leaman inductively coupled plasma (ICP) spectrometer. IR spectra were recorded on an Alpha Centauri FTIR spectrophotometer on pressed KBr pellets in the range $400\text{--}4000\text{ cm}^{-1}$. Water contents were determined by TG analyses on a PerkinElmer TGA7 instrument in flowing N_2 with a heating rate of $10\text{ }^{\circ}\text{C min}^{-1}$. Electrospray ionization mass spectrometry was carried out on a Bruker Micro TOF-QII instrument. X-ray photoelectron spectroscopy was performed on a VG ESCALABMKII spectrometer with an $\text{MgK}\alpha$ (1253.6 eV) achromatic X-ray source. The vacuum inside the analysis chamber was maintained at 6.2×10^{-6} Pa during the analysis. Magnetic measurements of the samples were performed on a Quantum Design PPMS-9. Data were corrected for the diamagnetic contribution calculated from Pascal constants.

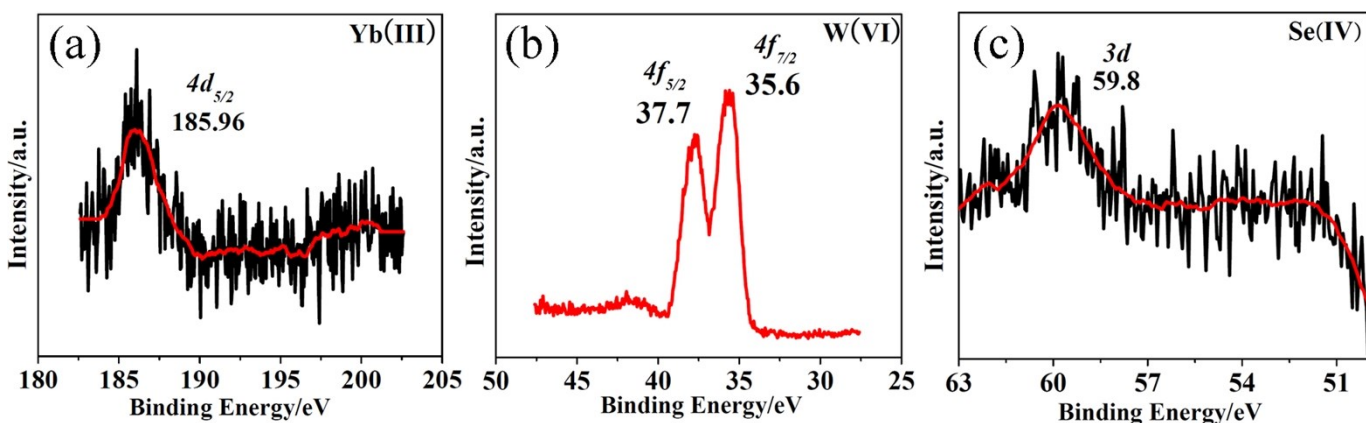


Fig. S7 Yb, W, and Se XPS spectra of 1.

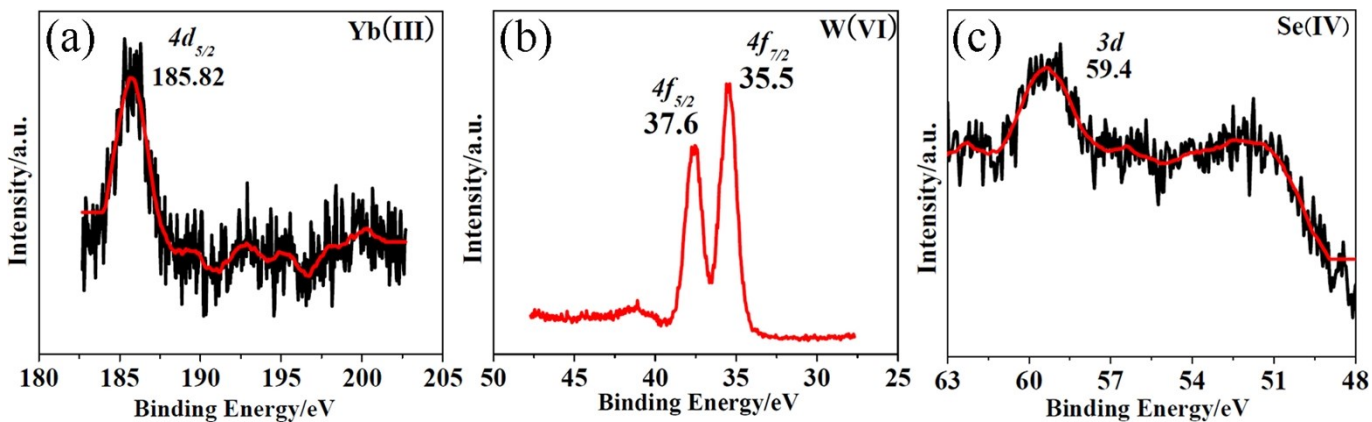


Fig. S8 Yb, W, and Se XPS spectra of 2.

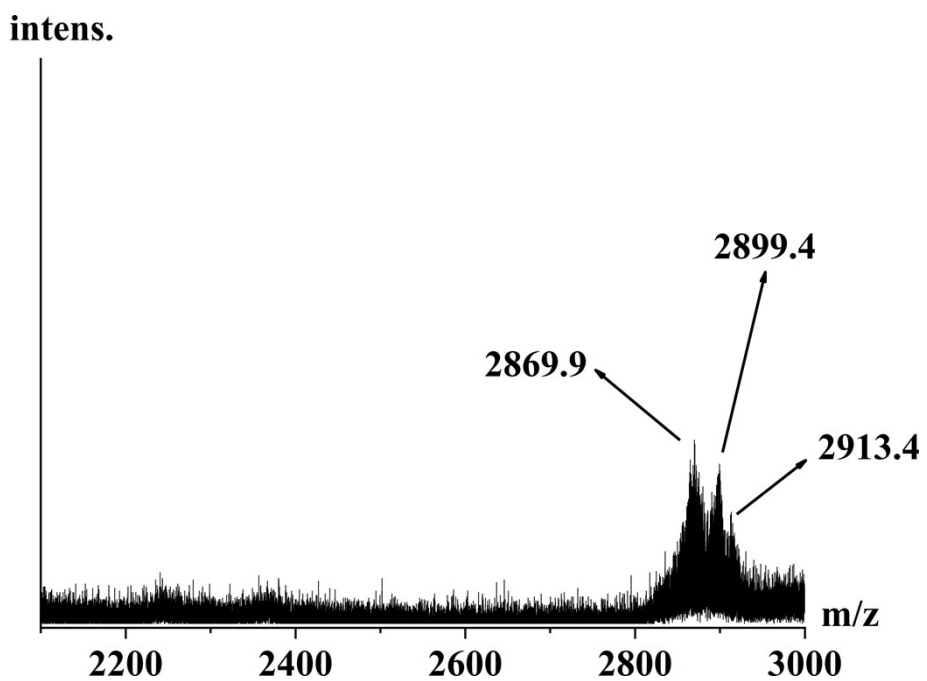


Table S7. Assignment of peaks of **1**.

Observed <i>m/z</i>	Calculated <i>m/z</i>	Charge	Molecular mass	Polyanion
2869.9	2869.8	-2	5739.7	$\{\text{NaH}_{10}[\text{Yb}_2\text{Se}_2\text{W}_{21}\text{O}_{76}(\text{H}_2\text{O})_6](\text{H}_2\text{O})\}^{2-}$
2899.4	2898.8	-2	5797.7	$\{\text{Na}_2\text{H}_9[\text{Yb}_2\text{Se}_2\text{W}_{21}\text{O}_{76}(\text{H}_2\text{O})_6](\text{H}_2\text{O})_3\}^{2-}$
2913.4	2913.8	-2	5827.7	$\{\text{Na}_5\text{H}_6[\text{Yb}_2\text{Se}_2\text{W}_{21}\text{O}_{76}(\text{H}_2\text{O})_6](\text{H}_2\text{O})\}^{2-}$

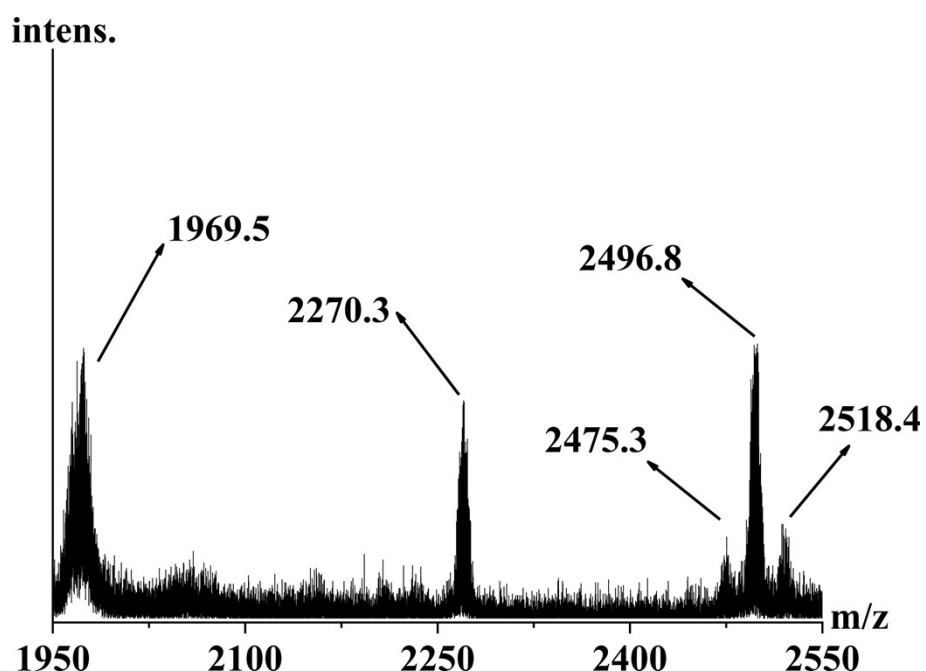


Fig. S10 ESI-MS of **2** in H_2O .

Table S8. Assignment of peaks of **2**.

Observed <i>m/z</i>	Calculated <i>m/z</i>	Charge	Molecular mass	Polyanion
1969.5	1969.9	-2	3939.8	$\{\text{Na}_{10}[\text{Se}_2\text{W}_{13}\text{O}_{49}(\text{H}_2\text{O})](\text{H}_2\text{O})_{20}\}^{2-}$
2270.3	2269.8	-2	4593.5	$\{\text{H}_3[\text{Yb}_2\text{Se}_2\text{W}_{16}\text{O}_{55}(\text{OH})_5(\text{H}_2\text{O})_6](\text{H}_2\text{O})\}^{2-}$
2475.3	2474.7	-2	4949.5	$\{\text{Na}_8\text{H}_3[\text{Yb}_2\text{Se}_2\text{W}_{16}\text{O}_{61}(\text{OH})(\text{H}_2\text{O})_4](\text{H}_2\text{O})_{14}\}^{2-}$
2496.8	2496.7	-2	4993.5	$\{\text{Na}_{10}\text{H}[\text{Yb}_2\text{Se}_2\text{W}_{16}\text{O}_{61}(\text{OH})(\text{H}_2\text{O})_4](\text{H}_2\text{O})_{14}\}^{2-}$
2518.4	2517.7	-2	5035.5	$\{\text{Na}_7\text{H}_4[\text{Yb}_2\text{Se}_2\text{W}_{16}\text{O}_{61}(\text{OH})(\text{H}_2\text{O})_4](\text{H}_2\text{O})_{20}\}^{2-}$

Supplementary Magnetic Characterizations

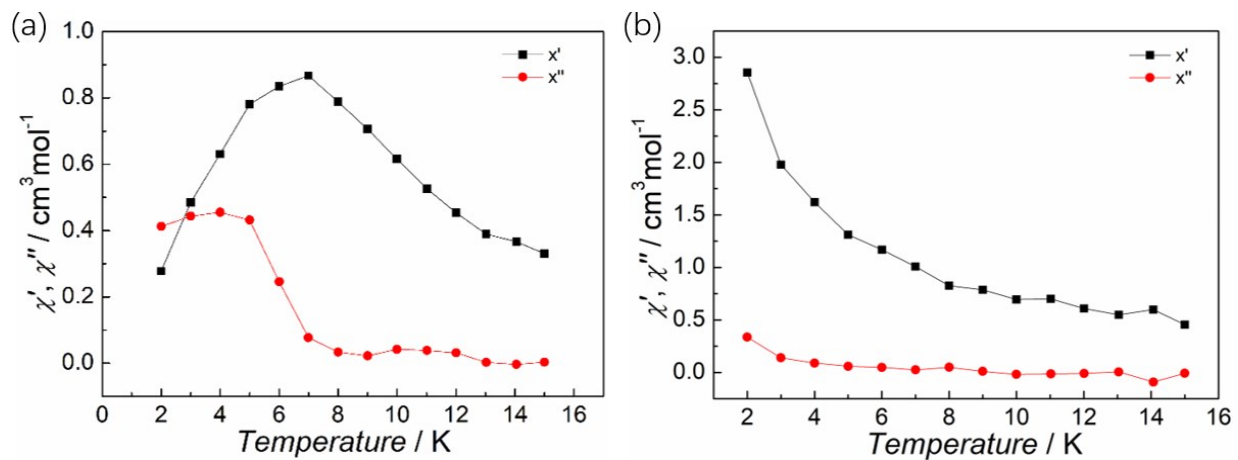


Fig. S11 Temperature dependences of the in-phase χ' and out-of-phase χ'' components of the ac susceptibility of **1** (a) and **2** (b) under an applied external dc field (2000 Oe) and a constant frequency (1000 Hz).

Table S9. Best fitted parameters (χ_T , χ_s , τ and α) with the generalized Debye model at 2000 Oe in the temperature range 2.5-8.0 K.

T / K	χ_T / cm ³ mol ⁻¹	χ_s / cm ³ mol ⁻¹	α	τ / s	R^2
2.5	2.24403	0.098	0.1609	9.13E-4	0.99687
3.0	2.08831	0.07656	0.1934	7.73E-4	0.9968
3.5	1.65605	0.07605	0.16133	4.47E-4	0.99592
4.0	1.38421	0.07609	0.11797	2.69E-4	0.98021
4.5	1.3633	0.05347	0.16531	2.19E-4	0.99759
5.0	1.12435	0.05704	0.11207	1.21E-4	0.9951
5.5	1.00169	0.06425	0.07498	7.43E-5	0.98155
6.0	0.93273	0.03324	0.10738	4.62E-5	0.98547
6.5	0.86314	0.02348	0.11418	2.94E-5	0.97896
7.0	0.78638	0.03337	0.0821	1.88E-5	0.9777
7.5	0.73609	0.01246	0.09245	1.25E-5	0.99333
8.0	0.69379	0.02271	0.09694	9.10E-6	0.99565

Section 4 Supplementary Physical Characterizations

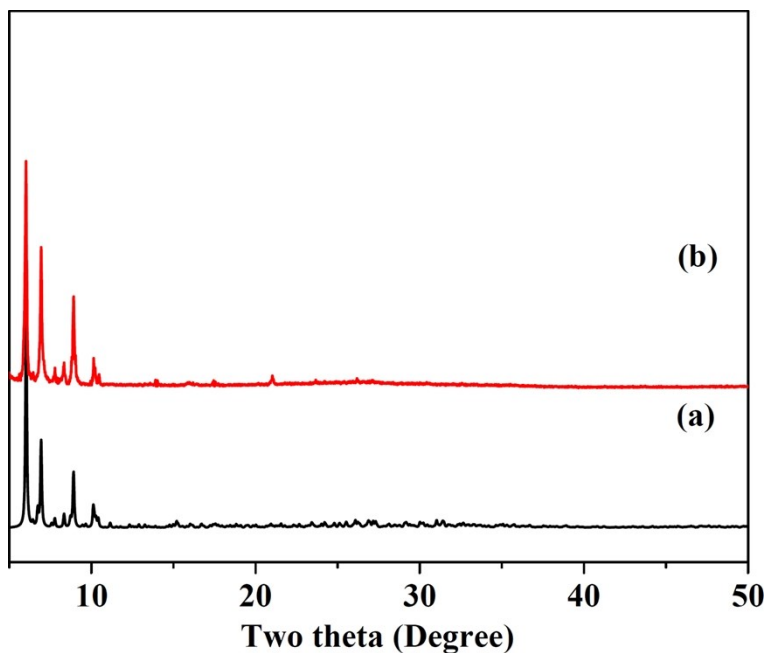


Fig. S12 The XRPD patterns of **1**: as-synthesized (b) and simulated (a).

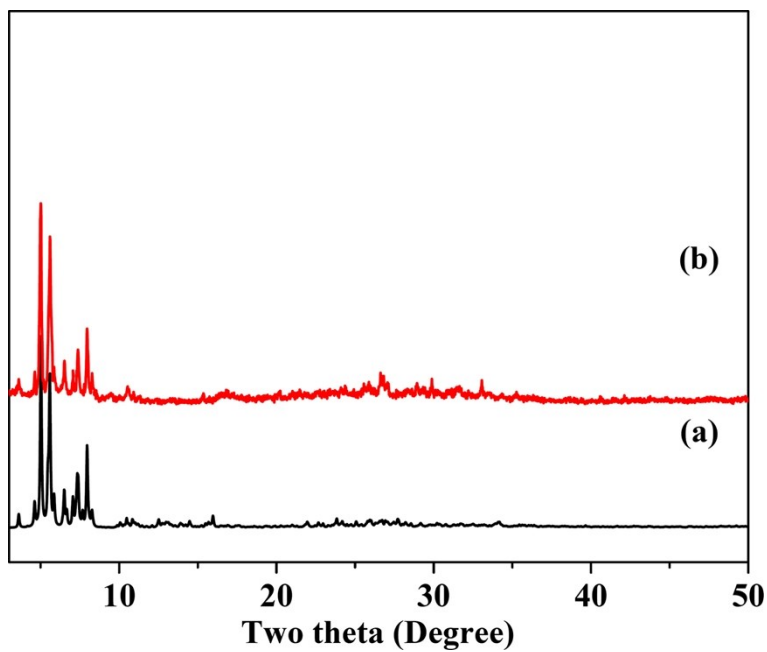


Fig. S13 The XRPD patterns of **2**: as-synthesized (b) and simulated (a).

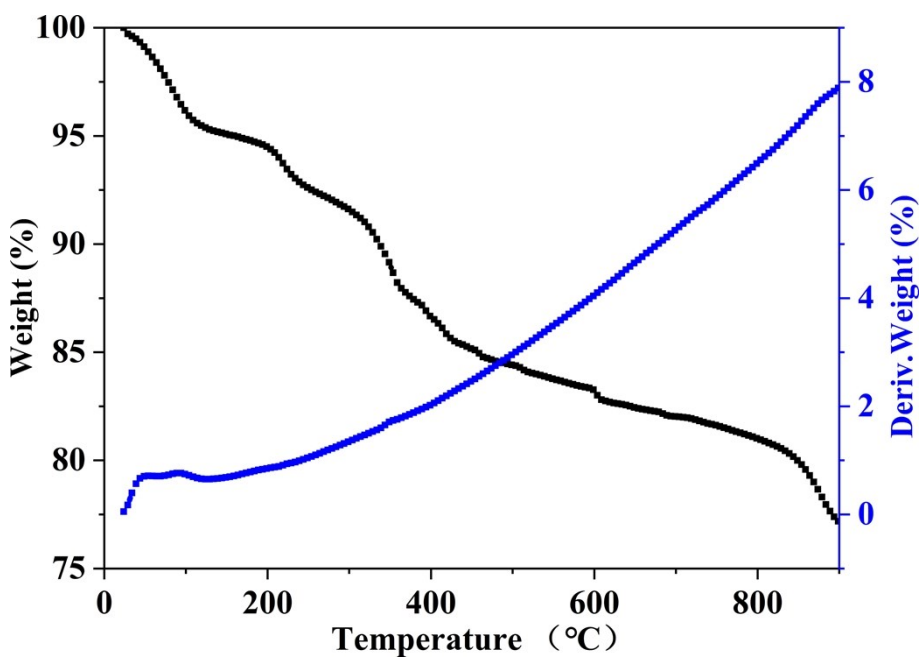


Fig. S14 TGA and DTA curves of **1**. The first and second weight loss is the lost of water molecules and organic amine groups (8.93 %). Then the structure begins to decompose.

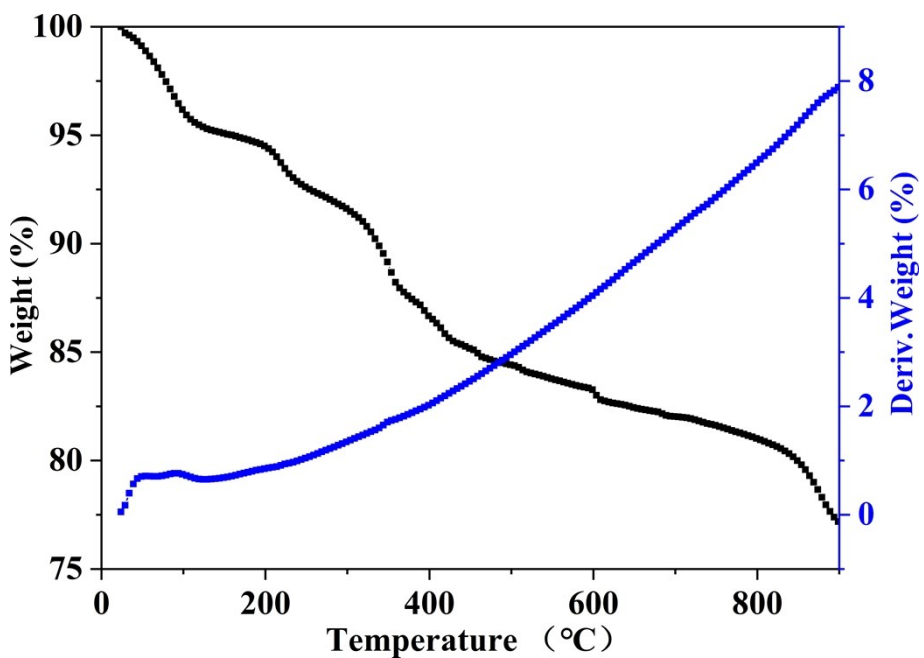


Fig. S15 TGA and DTA curves of **2**. The first and second weight loss is the lost of water molecules and organic amine groups (7.82 %). Then the structure begins to decompose.